Conformational Stability from Variable Temperature FT-IR Spectra of Krypton Solutions, r_0 Structural Parameters, Vibrational Assignment, and *ab Initio* Calculations of 4-Fluoro-1-butene

Gamil A. Guirgis,[†] Zhenhong Yu,[‡] Chao Zheng,[‡] Sarah Xiaohua Zhou,[‡] and James R. Durig*[,‡]

Department of Chemistry & Biochemistry, College of Charleston, Charleston, South Carolina 29424, and Department of Chemistry, University of Missouri−Kansas City, Kansas City, Missouri 64110

Received: June 20, 2007; In Final Form: December 14, 2007

Variable temperature (−115 to −155 °C) studies of the infrared spectra (3200−400 cm^{-1}) of 4-fluoro-1-butene, CH_2═$CHCH_2CH_2F$, dissolved in liquid krypton have been carried out. The infrared spectra of the gas and solid as well as the Raman spectra of the gas, liquid, and solid have also been recorded from 3200 to 100 cm^{-1}. From these data, an enthalpy difference of 72 ± 5 cm^{-1} (0.86 ± 0.06 $kJ·mol^{-1}$) has been determined between the most stable *skew−gauche II* conformer (the first designation refers to the position of the CH_2F group relative to the double bond, and the second designation refers to the relative positions of the fluorine atom to the C−C(═C) bond) and the second most stable *skew−trans* form. The third most stable conformer is the *skew−gauche I* with an enthalpy difference of 100 ± 7 cm^{-1} (1.20 ± 0.08 $kJ·mol^{-1}$) to the most stable form. Larger enthalpy values of 251 ± 12 cm^{-1} (3.00 ± 0.14 $kJ·mol^{-1}$) and 268 ± 17 cm^{-1} (3.21 ± 0.20 $kJ·mol^{-1}$) were obtained for the *cis−trans* and *cis−gauche* conformers, respectively. From these data and the relative statistical weights of one for the *cis−trans* conformer and two for all other forms, the following conformer percentages are calculated at 298 K: 36.4 ± 0.9% *skew−gauche II*, 25.7 ± 0.1% *skew−trans*, 22.5 ± 0.2% *skew−gauche I*, 10.0 ± 0.6% *cis−gauche*, and 5.4 ± 0.2% *cis−trans*. The potential surface describing the conformational interchange has been analyzed and the corresponding two-dimensional Fourier coefficients were obtained. Nearly complete vibrational assignments for the three most stable conformers are proposed and some fundamentals for the *cis−trans* and the *cis−gauche* conformers have been identified. The structural parameters, dipole moments, conformational stability, vibrational frequencies, infrared, and Raman intensities have been predicted from *ab initio* calculations and compared to the experimental values when applicable. The adjusted r_0 structural parameters have been determined by combining the *ab initio* predicted parameters with previously reported rotational constants from the microwave data. These experimental and theoretical results are compared to the corresponding quantities of some similar molecules.

Introduction

The conformational equilibria of 4-monosubstituted-1-butene molecules, CH_2═$CHCH_2CH_2X$, have been of interest to chemists for the past four decades. For 1-butene, where X = H, internal rotational isomerism involves only two forms, *cis* and *skew*.[1] An enthalpy difference of 2.2 ± 1.8 $kJ·mol^{-1}$ (185 ± 147 cm^{-1}) with the *skew* form more stable was reported[2] from a combined electron diffraction and microwave spectroscopic study with constraints taken from the optimized geometry of *ab initio* and molecular mechanics calculations. Recently, we[3] reported enthalpy differences of 0.87 ± 0.07 $kJ·mol^{-1}$ (73 ± 6 cm^{-1}) and 0.77 ± 0.12 $kJ·mol^{-1}$ (64 ± 10 cm^{-1}) from variable temperature studies of liquid krypton and xenon solutions, respectively, but both with the *cis* form more stable.

When X is other than hydrogen, rotation of the CH_2X group gives rise to the second conformational designation, *trans* (where X is antiperiplanar to the vinyl group), *gauche II* (where X is almost eclipsing the (═)C−H of the vinyl group), and *gauche I* (where X is pointing toward the double bond). Thus, a total of five conformations, *i.e.*, *skew−trans*, *skew−gauche I*, *skew−gauche II*, *cis−trans*, and *cis−gauche*, is possible for 4-monosubstituted-1-butene molecules (Figure 1). For 4-chloro-1-butene,[4] where X = Cl, percentage compositions of 41(9)% *skew−trans*, 47% *skew−gauche* (*I* and *II* combined), 8% *cis−trans*, and 4% *cis−gauche* were tentatively determined from an electron diffraction study at 23 °C. Conformational equilibrium of 4-bromo-1-butene[4] where X = Br is very similar, with reported compositions of 38(10)% *skew−trans*, 50% *skew−gauche* (*I* and *II* combined), 8% *cis−trans*, and 4% *cis−gauche* at 23 °C. For 1-pentene[5] where X = CH_3, four of the five expected conformers were observed in the microwave spectrum, and the relative intensities of the $3_{0,3} \leftarrow 2_{0,2}$ transitions were found to be in qualitative agreement with the zero-point corrected MP2/6-311G(d) relative stability order of *skew−gauche I* > *skew−trans* (60 cm^{-1}, 0.79 $kJ·mol^{-1}$) > *skew−gauche II* (257 cm^{-1}, 3.38 $kJ·mol^{-1}$) > *cis−trans* (337 cm^{-1}, 4.44 $kJ·mol^{-1}$). For 3-butenylsilane,[6] where X = SiH_3, the conformational stability order of *cis−trans* ≥ *skew−trans* > *skew−gauche I* > *skew−gauche II* was determined from variable temperature studies of the Raman spectra of the liquid sample with only the *cis−trans* form existing in the polycrystalline solid.

There have been two previously reported microwave spectroscopic investigations of 4-fluoro-1-butene[7,8] (Figure 1). The

* Corresponding author. Phone: 01 816-235-6038. Fax: 01 816-235-2290. E-mail: durigj@umkc.edu.
[†] College of Charleston.
[‡] University of Missouri−Kansas City.

10.1021/jp0748213 CCC: $40.75
Published on Web 02/26/2008

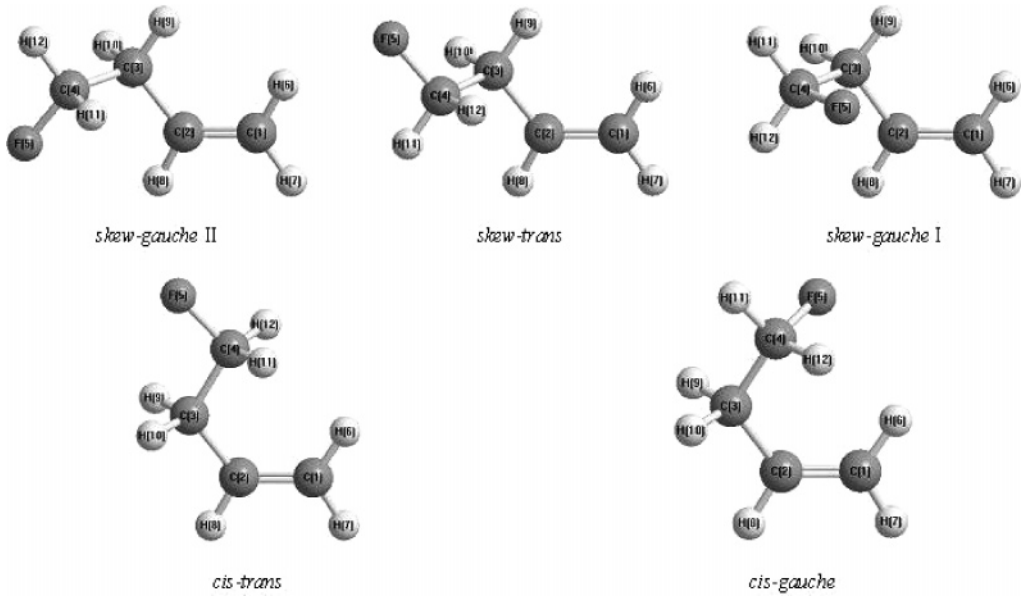

Figure 1. Stable *skew−gauche II*, *skew−trans*, *skew−gauche I*, *cis−gauche*, and *cis−trans* conformers of 4-fluoro-1-butene with atom numbering.

skew−trans conformer was the only form identified in the first microwave study[7] in the frequency region 26.5−40.0 GHz, and it was reported to be the predominant form. In the more recent microwave study of the frequency region 10.0−26.5 GHz, three of the five possible rotamers were identified with the *skew−gauche II* form reported[8] to be the most stable conformer. The *skew−trans* and the *skew−gauche I* forms were determined[8] to be less stable by 1.9 ± 0.2 kJ·mol^{-1} (159 ± 17 cm^{-1}) and 2.1 ± 0.2 kJ·mol^{-1} (176 ± 17 cm^{-1}), respectively. However, neither of the two *cis* forms has been identified and the apparent contradiction on the relative stability of the *skew−gauche II* and *skew−trans* forms between the results of the two microwave studies suggests that a reinvestigation of the conformational equilibrium of 4-fluoro-1-butene is desirable. Thus, as a continuation of the conformational study of this series of 4-monosubstituted-1-butene molecules, we recorded the variable temperature FT-IR spectra of 4-fluoro-1-butene in liquid krypton and determined the relative stabilities of all five conformers. The potential surface describing the conformational interchange has been analyzed and the corresponding two-dimensional Fourier coefficients were obtained. In addition, by systematically adjusting the *ab initio* MP2(full)/6-311+G(d,p) optimized structure to fit the previously reported microwave rotational constants,[7,8] r_0 structural parameters have been determined for the *skew−trans*, *skew−gauche II* and *skew−gauche I* forms and estimated for the *cis−trans* and the *cis−gauche* forms. The results of these vibrational and theoretical investigations are reported herein.

Experimental Section

The sample of 4-fluoro-1-butene was prepared by the reaction of 4-buten-1-ol with (diethylamino)sulfur trifluoride in diglyme for 2 h at −60 °C. The volatile material was collected and washed with water and 5% sodium bicarbonate. The sample was purified by using a low-temperature, low-pressure fractionation column, and the purity of the sample was checked by mass spectrometry and NMR spectroscopy. The purified sample was kept in the dark at low temperature until it was used. All sample transfers were carried out under vacuum to avoid contamination.

The mid-infrared spectra of the gas (Figure 2A) and the annealed solid (Figure 2B) from 3200 to 400 cm^{-1} were recorded on a Digilab model FTS-14C Fourier transform interferometer equipped with a Globar source, a Ge/KBr beamsplitter and a TGS detector. The spectrum of the gas was obtained with the sample contained in a 12 cm cell equipped with CsI windows. Atmospheric water vapor was removed from the interferometer chamber by purging with dry nitrogen. For the annealed solid, the spectrum was recorded by depositing a solid sample film onto a CsI substrate that was cooled by boiling liquid nitrogen and housed in a vacuum cell fitted with CsI windows. The sample was annealed until no further change was observed in the spectrum. A total of 128 and 64 scans were collected, averaged, and transformed with a boxcar truncation function for the gas and the solid, with resolutions of 0.5 and 2.0 cm^{-1}, respectively, to give a satisfactory signal-to-noise ratio.

The far-infrared spectrum of the gas (Figure 1S) from 380 to 80 cm^{-1} was recorded on a Nicolet model 200 SXV Fourier transform interferometer equipped with a vacuum bench, a Globar source, a liquid helium cooled germanium bolometer with a wedged sapphire filter and polyethylene windows. Traces of water were removed by passing the gaseous sample through activated 3 Å molecular sieves, using standard vacuum techniques. The gaseous sample was contained in a 1 m optical path cell with polyethylene windows. A 6.25 μm Mylar beamsplitter was used to record the spectra at a resolution of 0.1 cm^{-1}. Typically, 256 scans were needed for both the sample and reference, averaged, and transformed with a boxcar truncation function to give a satisfactory signal-to-noise ratio.

The far-infrared spectrum of the amorphous (Figure 3A) and the annealed solid (Figure 3B) from 540 to 60 cm^{-1} were recorded with a Perkin-Elmer model 2000 Fourier transform interferometer equipped with a far-infrared grid beamsplitter and a DTGS detector. The spectra were obtained by condensing the sample onto a silicon plate held in a cell equipped with polyethylene windows and cooled with boiling liquid nitrogen. The sample was annealed until no further changes were observed in the spectrum.

The mid-infrared spectra of the sample dissolved in liquefied krypton (Figure 4A) were recorded on a Bruker model IFS-66 Fourier interferometer equipped with a Globar source, a Ge/KBr beamsplitter and a DTGS detector. The spectra were recorded at variable temperatures ranging from −115 to −155 °C with 100 scans at a resolution of 1.0 cm^{-1}. The temperature

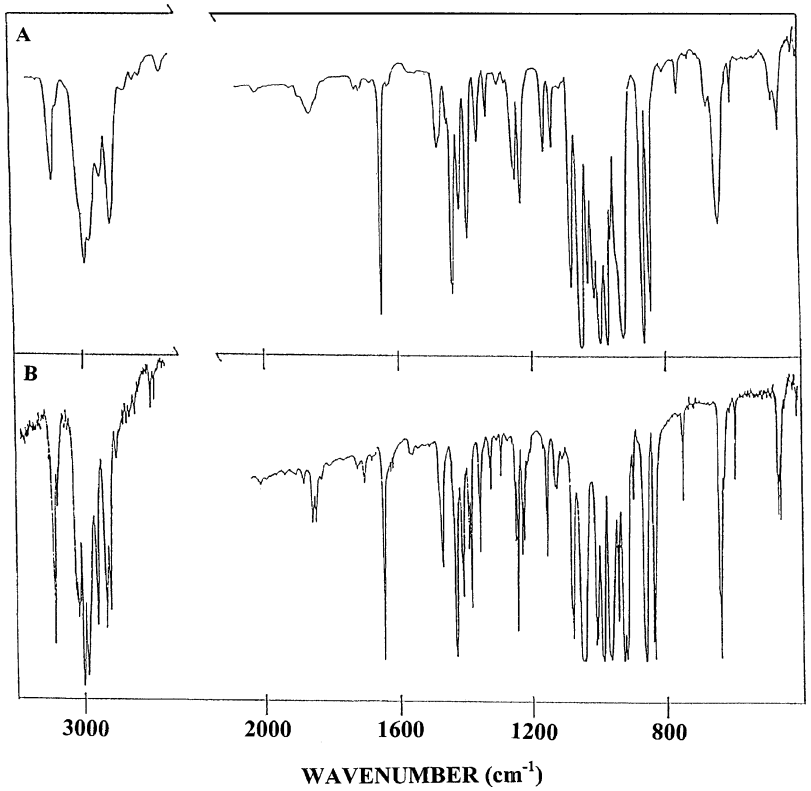

Figure 2. Mid-infrared spectra of 4-fluoro-1-butene: (A) gas; (B) annealed solid.

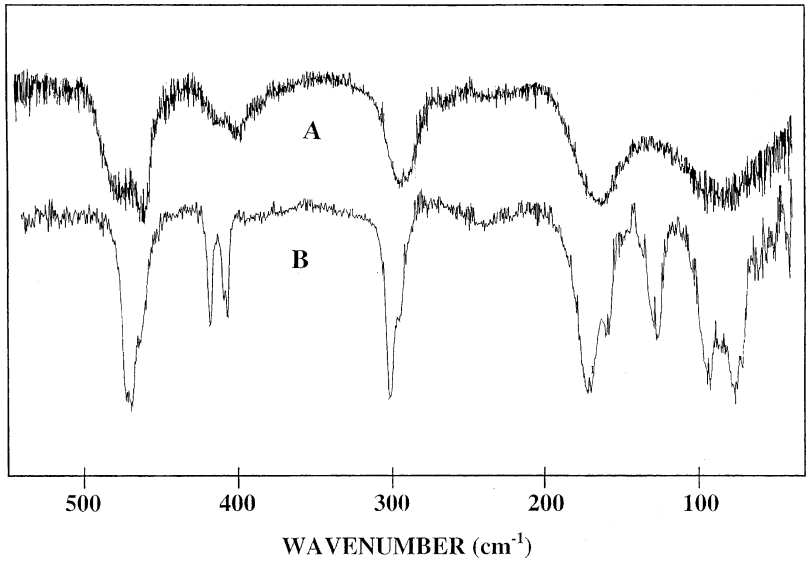

Figure 3. Far-infrared spectra of 4-fluoro-1-butene: (A) amorphous solid; (B) annealed solid.

studies in liquefied krypton were carried out in a specially designed cryostat cell, which is composed of a copper cell with a 4 cm path length and wedged silicon windows sealed to the cell with indium gaskets. The temperature was monitored by two platinum thermoresistors and the cell was cooled by boiling liquid nitrogen.

The Raman spectra (Figure 5) of 4-fluoro-1-butene from 3200 to 20 cm^{-1} were recorded on a Cary model 82 spectrophotometer equipped with a Spectra-Physics model 171 argon ion laser operating on the 5145 Å line. Laser power at the sample ranged from 0.4 to 2.0 W depending on the physical state of the sample. The spectrum of the gas (Figure 5A) was recorded with a standard Cary multipass accessory. The spectrum of the liquid (Figure 5B) was obtained from the sample sealed in a glass capillary that contained a spherical bulb on the end.[9] The spectrum of the annealed solid (Figure 5C) was obtained by condensing the sample on a blackened brass block, which was maintained in a cell fitted with quartz windows, cooled with boiling liquid nitrogen and annealed until no further changes in the spectrum were noted.

Ab Initio Calculations

The LCAO-MO-SCF calculations were performed with the Gaussian-03 program[10] by using Gaussian-type basis functions. The energy minima with respect to nuclear coordinates were obtained by simultaneous relaxation of all geometric parameters consistent with symmetry restrictions using the gradient method of Pulay.[11] Results from frequency calculations suggest that all five conformers, *i.e.*, *skew−gauche II*, *skew−trans*, *skew−*

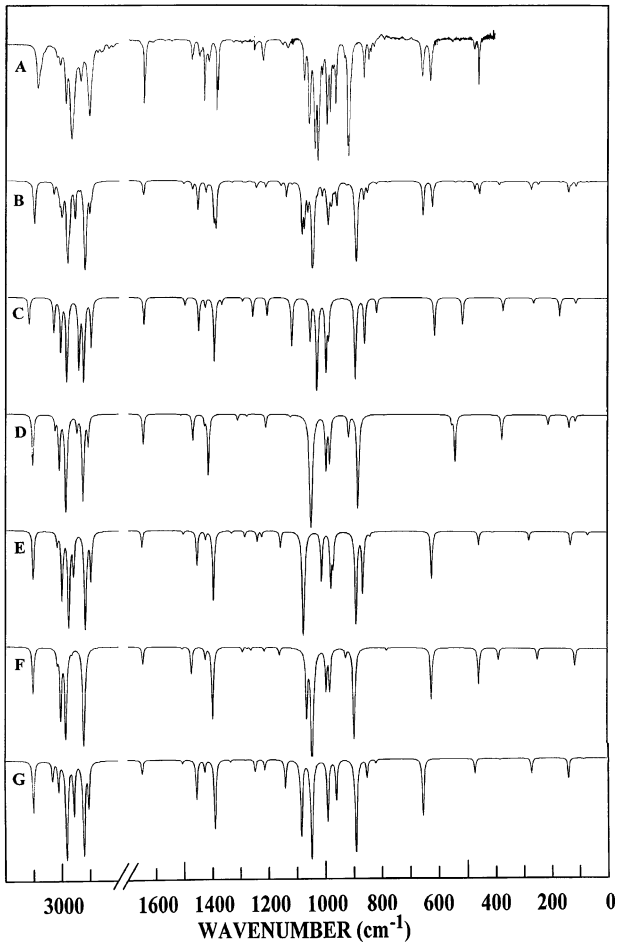

Figure 4. Infrared spectra of 4-fluoro-1-butene: (A) krypton solution at −130 °C; (B) simulated spectrum of a mixture of the five conformers at −130 °C with experimentally determined Δ*H* values listed in Table 6; (C) simulated spectrum for pure *cis*−*gauche* form; (D) simulated spectrum for pure *cis*−*trans* form; (E) simulated spectrum for pure *skew*−*gauche I* form; (F) simulated spectrum for pure *skew*−*trans* form; (G) simulated spectrum for pure *skew*−*gauche II* form.

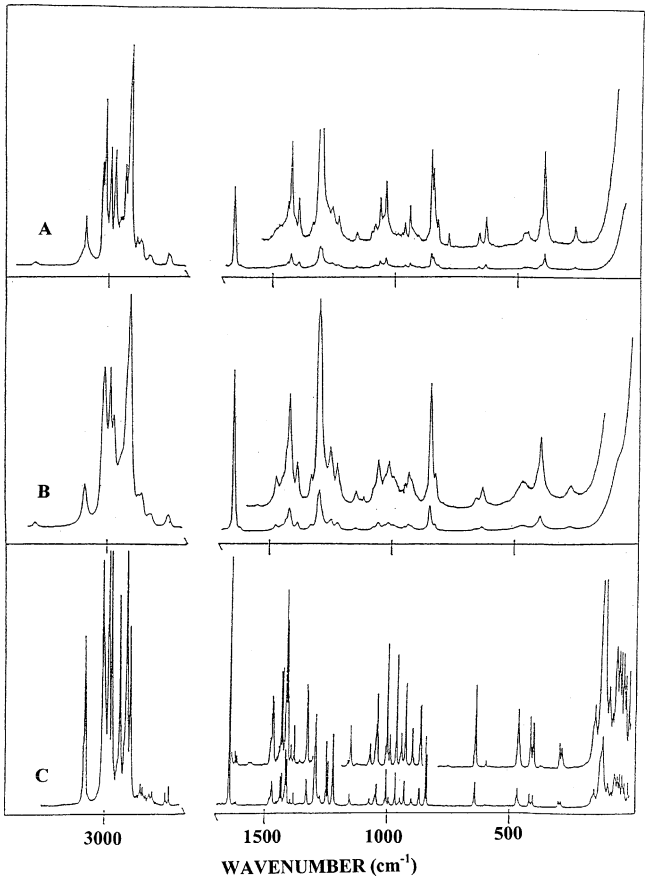

Figure 5. Raman spectra of 4-fluoro-1-butene: (A) gas; (B) liquid; (C) annealed solid.

gauche I, *cis*−*trans*, and *cis*−*gauche* (Figure 1), correspond to local minima on the potential surface. The predicted wavenumbers of the fundamentals of the three most stable conformers are listed in Tables 1−3, along with the observed values and for the two *cis* conformers in Tables 1S and 2S. Eight basis sets, from 6-31G(d) to 6-311+G(2df,2pd), were employed with Møller−Plesset perturbation theory[12] to the second order (MP2-(full)) as well as hybrid density functional theory by the B3LYP method,[13,14] to obtain energy differences among the stable conformers (Table 4). From all levels of calculation conducted in the present investigation, the *skew*−*gauche II* conformer is predicted to be the most stable form, the *skew*−*trans* conformer is predicted to be the second most stable form (both with exception from the B3LYP/6-31+G(d) calculation), and the *skew*−*gauche I* conformer is predicted to be the third most stable form. The *cis*−*trans* and the *cis*−*gauche* forms are predicted to be the two highest energy conformers. The values in Table 4 suggest that the inclusion of diffuse functions significantly lowers the predicted energies of the CCCF *trans* orientation and raises the energies of the CCCF *gauche* orientation.

To obtain a more complete description of the nuclear motions involved in the vibrational fundamentals of 4-fluoro-1-butene, normal coordinate analyses have been carried out. The force fields in Cartesian coordinates were obtained by the Gaussian-03 program[10] at the MP2(full)/6-31G(d) level. The internal coordinates used to calculate the **G** and **B** matrices are listed along with the structural parameters in Table 5, and the numbering is shown in Figure 1. With the **B** matrix, the force field in Cartesian coordinates was converted to a force field in internal coordinates[15] in which the pure *ab initio* vibrational frequencies were reproduced. Subsequently, scaling factors of 0.88 for the CH stretches and 0.90 for all other modes except the heavy atoms (1.0) were used, along with the geometric average of scaling factors for interaction force constants, to obtain the fixed scaled force field (Table 3S) and the resultant wavenumbers. A set of symmetry coordinates was used (Table 4S) to determine the corresponding potential energy distributions (PEDs), which are listed in Tables 1−3 for the three most stable conformers and for the *cis*−*trans* and *cis*−*gauche* forms in Tables 1S and 2S, respectively.

To identify the fundamental vibrations for the five conformers of 4-fluoro-1-butene, the infrared spectra were predicted using fixed scaled frequencies. Infrared intensities obtained from MP2-(full)/6-31G(d) calculations based on the dipole moment derivatives with respect to Cartesian coordinates were transformed with respect to normal coordinates by $(\partial\mu_u/\partial Q_i) = \sum_j (\partial\mu_u/\partial X_j) L_{ij}$ as previously described.[15] In Figure 4G,F,E,D,C, the simulated infrared spectra of the pure *skew*−*gauche II*, *skew*−*trans*, *skew*−*gauche I*, *cis*−*trans* and *cis*−*gauche* conformers, respectively, are shown. The simulated spectra calculated at −130 °C, of a mixture of five conformers with Δ*H* values of 72, 100, 251, and 268 cm^{-1} (experimentally determined values, see Conformational Stability section), respectively, is shown in Figure 4B, and it should be compared to the experimental spectrum of the krypton solution at −130 °C (Figure 4A). The predicted spectrum is in good agreement with the experimental

TABLE 1: Observed and Calculated Frequencies (cm^{-1}) and Potential Energy Distributions (PEDs) for the *Skew−Gauche II* Conformer of 4-Fluoro-1-butene

	description[f]	*ab initio*[a]	fixed scaled[b]	IR int[c]	Raman act.[d]	IR gas	Raman gas	IR liq Kr	Raman liq	contour A	contour B	contour C	PED[e]
ν_1	$=CH_2$ antisymmetric stretch	3304	3100	14.0	59.0	3094	3094	3087	3087	5	94	1	$97S_1$
ν_2	=CH stretch	3232	3032	4.4	85.6	3004	3016	3009	3013	4	91	5	$93S_2$
ν_3	$=CH_2$ symmetric stretch	3210	3011	7.0	61.4		2995	2988	2988	61	28	11	$94S_3$
ν_4	$*CH_2$ antisymmetric stretch	3180	2982	45.2	55.0	2970	2975	2967	2972	28	17	55	$95S_4$
ν_5	CH_2 antisymmetric stretch	3151	2956	14.6	66.4		2933	2935	2940	1	62	37	$94S_5$
ν_6	$*CH_2$ symmetric stretch	3114	2921	39.7	124.0	2911	2914		2910	33	39	28	$97S_6$
ν_7	CH_2 symmetric stretch	3096	2904	11.5	72.7			2904		0	53	47	$98S_7$
ν_8	C=C stretch	1737	1648	3.1	5.6	1649	1651	1648	1650	88	1	11	$67S_8$, $15S_{11}$
ν_9	$*CH_2$ deformation	1585	1505	0.8	9.1	1479	1476	1478	1477	44	48	8	$99S_9$
ν_{10}	CH_2 deformation	1533	1455	9.9	8.0	1437	1441	1432	1432	38	54	8	$88S_{10}$
ν_{11}	$=CH_2$ deformation	1503	1426	2.6	13.0	1412	1412	1416	1420	34	16	50	$65S_{11}$, $11S_{10}$
ν_{12}	$*CH_2$ wag	1465	1390	21.4	4.5	1393	1390	1384	1388	66	33	1	$88S_{12}$
ν_{13}	CH_2 wag	1406	1334	0.5	4.3			1335		14	29	57	$60S_{13}$, $12S_{16}$
ν_{14}	=CH in-plane bend	1350	1281	0.1	17.2	1299	1296	1296	1300	94	6	0	$63S_{14}$, $15S_8$
ν_{15}	CH_2 twist	1312	1247	2.7	13.4		1257	1255	1255	52	38	10	$36S_{15}$, $27S_{16}$, $12S_{13}$
ν_{16}	$*CH_2$ twist	1277	1213	2.2	5.6	1222		1224	1229	26	2	72	$48S_{16}$, $26S_{15}$, $16S_{18}$
ν_{17}	C−C stretch	1193	1140	6.6	1.5	1140	1143	1138	1138	46	20	34	$19S_{17}$, $19S_{24}$, $18S_{21}$
ν_{18}	$*CH_2$ rock	1138	1084	25.4	3.8	1088	1085	1078	1080	18	75	7	$29S_{18}$, $27S_{19}$, $17S_{23}$
ν_{19}	*C−F stretch	1104	1048	46.4	2.8	1037	1038	1038	1033	50	48	2	$36S_{19}$, $17S_{18}$
ν_{20}	$=CH_2$ twist	1044	991	18.0	0.6	996		996	999	9	0	91	$64S_{20}$, $31S_{25}$
ν_{21}	$=CH_2$ wag	1011	961	10.1	2.4	961	961	965	951	28	54	18	$35S_{21}$, $17S_{19}$, $16S_{23}$
ν_{22}	$=CH_2$ rock	941	892	37.9	0.03	922		918		11	2	87	$99S_{22}$
ν_{23}	*C−C stretch	898	853	4.0	6.3		852	850		2	85	13	$27S_{23}$, $21S_{21}$, $17S_{17}$, $12S_{19}$, $11S_{24}$
ν_{24}	CH_2 rock	865	822	0.8	1.6		825	830	825	2	93	5	$35S_{24}$, $25S_{17}$, $18S_{18}$
ν_{25}	=CH out-of-plane bend	686	655	16.1	6.7	655	659	657	660	30	1	69	$39S_{25}$, $27S_{20}$, $12S_{28}$
ν_{26}	C*CF bend	488	474	3.3	4.2	474	474	474	470	98	1	1	$34S_{26}$, $15S_{27}$, $15S_{24}$, $10S_{28}$
ν_{27}	C=C−C bend	395	387	0.2	2.2	396	393		396	17	82	1	$62S_{27}$, $16S_{26}$
ν_{28}	*C−C−C bend	280	274	3.3	2.3	279	270		277	24	6	70	$49S_{28}$, $25S_{26}$, $12S_{29}$
ν_{29}	$*CH_2F$ torsion	148	141	4.5	1.2	167				70	23	7	$65S_{29}$, $13S_{30}$
ν_{30}	asymmetric torsion	92	87	0.2	6.6	129				5	6	89	$76S_{30}$, $13S_{29}$

[a] Frequencies from MP2(full)/6-31G(d) calculation. [b] Scaling factors of 0.88 for CH stretches, 1.0 for heavy atom bends, and 0.90 for all other modes. [c] Calculated infrared intensities in km/mol. [d] Calculated Raman activities in $Å^4$/u. [e] Values less than 10% are omitted. [f] * indicates carbon atom in the CH_2F group.

spectrum, which indicates the utility of the scaled predicted data in distinguishing the fundamentals for the five conformers.

To further support the vibrational assignments, we have simulated the Raman spectra from the *ab initio* MP2(full)/6-31G(d) by utilizing the predicted Raman activities, scaled wavenumbers, and Lorentzian line function. The simulated Raman spectra of the pure *skew−gauche II*, *skew−trans*, *skew−gauche I*, *cis−trans*, and *cis−gauche* conformers are shown in Figure 6G,F,E,D,C, respectively. The simulated Raman spectra, calculated for 25 °C, of a mixture of five conformers with the experimentally determined ΔH values are shown in Figure 6B. The experimental Raman spectrum of the liquid is shown in Figure 6A for comparison, and the agreement is considered satisfactory, but not nearly as good as the corresponding simulated infrared spectrum, probably due, in part, to intermolecular association in the liquid phase. Additionally, the *ab initio* predictions of Raman spectral activities are not usually as good as the predictions of the corresponding infrared intensities.

Vibrational Assignment

To determine the relative conformation stabilities of the five conformers of 4-fluoro-1-1butene, it is necessary first to assign bands to each conformer. Because most fundamental vibrations of the five conformers have nearly the same predicted force constants and consequently frequencies, only the lower frequency bending modes have sufficient wavenumber differences for confident assignment to the individual conformer. Starting at this point, the most obvious assignments were made. The *cis−trans* and *cis−gauche* conformers have a fundamental predicted at 541 (observed 551) and 516 (observed 525) cm^{-1}, respectively, with no predicted bands for the three skew conformer for which they could be assigned. These bands are the ν_{25} fundamentals for both *cis* conformers with good predicted intensities, and both bands disappear from the infrared spectrum of the solid.

The corresponding fundamentals for the three skew conformers are predicted in the frequency range 600−700 cm^{-1}. In the infrared spectra of 4-fluoro-1-butene dissolved in liquid krypton, two strong bands at 657 and 628 cm^{-1} are observed, which correspond to the two pronounced Q-branches at 655 and 628 cm^{-1} in the infrared spectrum of the gas (660 and 632 cm^{-1} Raman spectrum of the liquid). The ν_{25} (=CH out-of-plane bend) fundamental is predicted (after scaling) at 655 cm^{-1} for the *skew−gauche II* conformer whereas the same mode is predicted at a significantly lower frequency at 622 cm^{-1} for both the *skew−trans* and the *skew−gauche I* forms. On the basis of the comparison of the predicted observed frequencies and relative intensities, the higher frequency band (655 cm^{-1}) is assigned to the *skew−gauche II* conformer. The 628 cm^{-1} band is then assigned to both of the other skew conformers. The relative intensities of these two strong bands is in complete agreement with the predicted values (Figure 2S).

Two bands are observed at 474 and 458 cm^{-1} in the infrared spectra of the krypton solution. The *skew−gauche II*, *skew−trans*, and *skew−gauche I* have fundamentals predicted at 474, 457, and 458 cm^{-1}, respectively, Thus the higher frequency band is assigned to the *skew−gauche II* form with the 458 cm^{-1} band assigned to the corresponding fundamental for the other two skew forms. The three skew conformers are predicted to have a fundamental near 400 cm^{-1} with two of them having nearly

TABLE 2: Observed and Calculated Frequencies (cm^{-1}) and Potential Energy Distributions (PEDs) for the *Skew−Trans* Conformer of 4-Fluoro-1-butene

	description[f]	*ab initio*[a]	fixed scaled[b]	IR int[c]	Raman act.[d]	IR gas	Raman gas	IR liq Kr	Raman liq	contour A	contour B	contour C	PED[e]
ν_1	$=CH_2$ antisymmetric stretch	3307	3102	12.4	58.0	3094	3094	3087	3087	38	51	11	$98S_1$
ν_2	=CH stretch	3202	3004	23.3	20.8		2995	2988	2988	0	51	49	$77S_2$, $18S_3$
ν_3	$=CH_2$ symmetric stretch	3216	3017	2.8	128.0		2995	2988	2988	94	6	0	$80S_3$, $17S_2$
ν_4	$*CH_2$ antisymmetric stretch	3183	2986	38.0	10.2	2970	2975	2967	2972	3	10	87	$69S_4$, $25S_5$
ν_5	CH_2 antisymmetric stretch	3161	2965	0.7	104.4		2933	2935	2940	2	4	94	$68S_5$, $28S_4$
ν_6	$*CH_2$ symmetric stretch	3115	2922	45.8	21.8	2911				1	89	10	$82S_6$, $17S_7$
ν_7	CH_2 symmetric stretch	3107	2915	2.5	144.3	2911	2914		2910	66	5	29	$81S_7$, $18S_6$
ν_8	C=C stretch	1736	1647	3.9	5.5	1649	1651	1648	1650	77	1	22	$67S_8$, $15S_{11}$
ν_9	$*CH_2$ deformation	1589	1508	0.4	6.6	1479	1476	1478	1477	87	4	9	$97S_9$
ν_{10}	CH_2 deformation	1553	1474	6.3	13.9	1457	1454	1450	1453	6	94	0	$93S_{10}$
ν_{11}	$=CH_2$ deformation	1502	1425	2.5	11.3	1412	1412	1616	1420	24	20	56	$69S_{11}$
ν_{12}	$*CH_2$ wag	1473	1398	23.2	3.0	1393	1390	1388	1388	98	1	1	$78S_{12}$, $10S_{13}$
ν_{13}	CH_2 wag	1329	1263	0.6	6.0		1279			4	96	0	$60S_{13}$, $14S_{12}$, $13S_{14}$
ν_{14}	=CH in-plane bend	1362	1293	1.0	3.8	1306	1304	1302	1300	40	24	36	$47S_{14}$, $14S_8$
ν_{15}	CH_2 twist	1279	1215	0.8	0.7	1222		1224	1229	3	7	90	$33S_{15}$, $34S_{16}$, $17S_{18}$
ν_{16}	$*CH_2$ twist	1346	1277	0.3	23.2		1287			2	43	55	$43S_{16}$, $31S_{15}$
ν_{17}	C−C stretch	1049	995	10.7	0.1	996		996	999	7	69	24	$13S_{17}$, $22S_{25}$, $22S_{20}$
ν_{18}	$*CH_2$ rock	1219	1161	1.6	4.7	1159	1158	1156	1156	0	32	68	$29S_{18}$, $19S_{24}$, $17S_{21}$, $13S_{17}$
ν_{19}	*C−F stretch	1096	1044	82.9	7.0	1037	1038	1038	1033	85	15	0	$83S_{19}$
ν_{20}	$=CH_2$ twist	1035	982	10.8	0.9	988	990	985		13	6	81	$42S_{20}$, $13S_{25}$, $10S_{17}$
ν_{21}	$=CH_2$ wag	974	927	1.8	1.6		940	936	936	99	0	1	$47S_{21}$, $31S_{17}$
ν_{22}	$=CH_2$ rock	944	896	37.0	0.03	922		922		11	35	54	$98S_{22}$
ν_{23}	*C−C stretch	1115	1064	21.2	6.7	1061	1062	1061	1061	100	0	0	$71S_{23}$
ν_{24}	CH_2 rock	823	781	0.5	0.1	793	792	794		25	75	0	$44S_{24}$, $30S_{18}$
ν_{25}	=CH out-of-plane bend	653	622	13.9	8.4	628		628	632	7	35	58	$45S_{25}$, $30S_{20}$
ν_{26}	C*CF bend	398	388	2.5	4.0	396	393		396	65	9	26	$22S_{26}$, $28S_{27}$, $15S_{28}$
ν_{27}	C=C−C bend	467	457	8.9	0.8	468	468	458		82	15	3	$47S_{27}$, $33S_{26}$
ν_{28}	*C−C−C bend	254	250	2.5	3.8	270			277	25	52	23	$54S_{28}$, $26S_{26}$
ν_{29}	$*CH_2F$ torsion	121	115	3.8	0.8	146				4	30	66	$81S_{29}$
ν_{30}	asymmetric torsion	89	85	0.1	4.8	129				42	12	46	$79S_{30}$

[a] Frequencies from MP2(full)/6-31G(d) calculation. [b] Scaling factors of 0.88 for CH stretches, 1.0 for heavy atom bends, and 0.90 for all other modes. [c] Calculated infrared intensities in km/mol. [d] Calculated Raman activities in $Å^4$/u. [e] Values less than 10% are omitted. [f] * indicates carbon atom in the CH_2F group.

the same frequency for this normal mode. Two bands are observed at 410 and 396 cm^{-1} (infrared gas) with the 410 cm^{-1} band assigned to the *skew−gauche I* conformer on the basis of the predicted frequencies for this mode for the three skew conformers.

Confident assignments can also be made for the five bands at 866, 850, 842, 830, and 794 cm^{-1}, which were observed in the infrared spectra of the krypton solutions. Two fundamentals at 853 and 822 cm^{-1} and 866 and 842 cm^{-1} are predicted for the *skew−gauche II* and *skew−gauche I* forms, respectively, whereas only one fundamental at 781 cm^{-1} is predicted for the *skew−trans* form. Thus, the assignments for these five bands follow directly from the predicted frequencies and is supported by the relative intensities and hybrid band contours in the spectrum of the gas.

There is a relatively large number of fundamentals between 900 and 1100 cm^{-1}, which makes their assignment much more difficult and many of the bands are due to fundamentals of two conformers (Figure 7). Therefore, there were only two bands in this spectral region that could be confidently used for enthalpy determination, and they are the bands at 965 cm^{-1} (*skew−gauche II*) and 1061 cm^{-1} (*skew−trans*).

These assignments now permit the identification of several bands that are confidently assigned to fundamental modes that arise from the vibration of one conformer and can, thus, be used for the enthalpy determinations. Also, using all of these data, along with well-characterized "group frequency" information, has provided nearly complete vibrational assignments for the fundamental vibrations for the three *skew* conformers (Tables 1−3) and a few bands are confidently assigned to the two *cis* forms (Tables 1S and 2S).

Most of the bands observed in the infrared and Raman spectra of the solid appear as doublets and this is probably a result of two molecules per primitive cell in the crystal structure. The spectral bands assigned to the *cis−trans*, *cis−gauche*, and *skew−trans* in the fluid phases are not present in the spectra of the solid. However it is difficult to distinguish whether the *skew−gauche I* or *skew−gauche II* form is in the solid but the spectral data favor the *skew−gauche I* form. The two bands observed at 393 and 411 cm^{-1} in the infrared spectrum of the gas remain in the spectrum of the solid as a doublet at 417/406 cm^{-1}, which comes from the 411 cm^{-1} band assigned to the *skew−gauche I* conformer. The two doublets at 868/862 and 842/836 cm^{-1} arise from the 866 and 842 cm^{-1} bands (gas), which were assigned as *skew−gauche I* modes. The single band at 639 cm^{-1} in the spectrum of the solid can also be reasonably assigned to the *skew−gauche* I form. The fact that the most stable form in the fluid phases is probably not the conformer in the solid is not surprising when the ΔH value between them is only 100 ± 10 cm^{-1}. The packing in the crystal could readily be the reason for the change in the conformer stability.

Conformational Stability

To determine the enthalpy differences among the five conformers, the mid-infrared spectra of 4-fluoro-1-butene dissolved in liquefied krypton as a function of temperature, from −115 to −155 °C, were recorded. Only small interactions are expected to occur between the dissolved sample and the surrounding krypton atoms, and consequently, only small frequency shifts are anticipated when passing from the gas phase to the liquefied krypton solutions.[20−24] A significant advantage

TABLE 3: Observed and Calculated Frequencies (cm^{-1}) and Potential Energy Distributions (PEDs) for the *Skew*−*Gauche* I Conformer of 4-Fluoro-1-butene

	description[f]	*ab initio*[a]	fixed scaled[b]	IR int[c]	Raman act.[d]	IR gas	Raman gas	IR liq Kr	Raman liq	IR solid	Raman solid	contour A	contour B	contour C	PED[e]
ν_1	$=CH_2$ antisymmetric stretch	3308	3103	12.9	57.9	3094	3094	3087	3087	3078	3080	24	3	73	$99S_1$
ν_2	=CH stretch	3198	3000	21.5	29.8	3004	3016	3009	3013	3010	3009	0	5	95	$86S_2$, $10S_3$
ν_3	$=CH_2$ symmetric stretch	3217	3018	2.9	119.8		2995	2988	2988	2988	2984	76	24	0	$88S_3$
ν_4	$*CH_2$ antisymmetric stretch	3172	2976	42.4	46.4	2970	2975	2967		2975	2973	16	2	82	$86S_4$, $10S_5$
ν_5	CH_2 antisymmetric stretch	3154	2959	10.5	78.3		2933	2935	2940	2941	2940	28	69	3	$78S_5$, $13S_4$
ν_6	$*CH_2$ symmetric stretch	3110	2917	45.0	121.8	2911				2915	2913	50	39	11	$96S_6$
ν_7	CH_2 symmetric stretch	3089	2897	12.7	76.2		2914	2904	2910	2900	2900	1	72	27	$87S_7$
ν_8	C=C stretch	1740	1651	3.7	5.3	1652	1651	1648	1650	1645	1645	61	33	6	$67S_8$, $15S_{11}$
ν_9	$*CH_2$ deformation	1585	1504	0.7	10.3	1479	1476	1478	1477	1473/1471	1473/1470	12	79	9	$99S_9$
ν_{10}	CH_2 deformation	1534	1455	8.4	7.3	1437	1441	1432	1432	1434/1431	1438/1431	22	8	70	$87S_{10}$
ν_{11}	$=CH_2$ deformation	1501	1425	1.7	12.6	1412	1412	1416	1420	1415/1411	1417/1411	1	91	8	$65S_{11}$, $12S_{10}$
ν_{12}	$*CH_2$ wag	1472	1396	21.4	3.1	1393	1390	1388	1388	1394/1386	1396/1384	39	61	0	$89S_{12}$
ν_{13}	CH_2 wag	1404	1332	0.5	4.2		1335					8	79	13	$62S_{13}$, $13S_{16}$
ν_{14}	=CH in-plane bend	1354	1285	1.3	12.8		1304		1300	1297	1299/1295	46	12	42	$65S_{14}$, $14S_8$, $11S_{21}$
ν_{15}	CH_2 twist	1289	1225	1.2	7.2	1231	1234			1231/1225	1227	13	12	75	$39S_{15}$, $25S_{16}$
ν_{16}	$*CH_2$ twist	1306	1241	2.3	19.9		1257	1255	1255	1252/1244	1253/1246	73	26	1	$45S_{16}$, $32S_{15}$
ν_{17}	C−C stretch	888	842	0.8	5.7		845	842	846	842/836	842/836	4	96	0	$37S_{17}$, $21S_{23}$, $14S_{18}$, $13S_{21}$
ν_{18}	$*CH_2$ rock	1214	1158	3.6	1.6		1158	1156	1156	1155	1158	4	18	78	$33S_{18}$, $14S_{21}$, $14S_{24}$, $12S_{17}$
ν_{19}	*C−F stretch	1133	1076	54.2	5.8	1088	1085	1078	1080	1083/1078	1075	12	88	0	$59S_{19}$, $26S_{23}$
ν_{20}	$=CH_2$ twist	1032	979	15.1	0.7	986		985		1010/1006	1004	29	71	0	$62S_{20}$, $26S_{25}$
ν_{21}	$=CH_2$ wag	1022	971	7.8	0.3	970	971	975		969/965	966	0	99	1	$38S_{21}$, $25S_{18}$, $10S_{14}$
ν_{22}	$=CH_2$ rock	938	890	37.8	0.02	922		918		929/918	927	39	58	3	$98S_{22}$
ν_{23}	*C−C stretch	1062	1012	13.2	2.0	1032		1027	1017	1049/1042	1049/1045	40	41	19	$18S_{23}$, $16S_{17}$, $14S_{24}$, $13S_{19}$
ν_{24}	CH_2 rock	910	866	17.7	3.5	862		866		868/862	869/864	27	73	0	$38S_{24}$, $20S_{19}$
ν_{25}	=CH out-of-plane bend	652	622	12.5	7.5	628	630	628	632	639	641	48	51	1	$35S_{25}$, $23S_{20}$, $13S_{24}$
ν_{26}	C*CF bend	470	458	3.0	4.5	458	457	458		462	468	90	9	1	$27S_{26}$, $28S_{27}$, $15S_{28}$, $10S_{25}$
ν_{27}	C=C−C bend	420	410	0.2	1.5	411	410			417/406	418/406	38	32	30	$40S_{27}$, $31S_{26}$
ν_{28}	*C−C−C bend	286	280	1.8	1.8	270	272		277	300	302/292	61	3	36	$48S_{28}$, $17S_{26}$, $13S_{27}$
ν_{29}	$*CH_2F$ torsion	138	132	2.9	1.9	158				172/159	165/158	61	1	38	$81S_{29}$
ν_{30}	asymmetric torsion	75	71	0.7	5.8	120				126	126	53	10	37	$85S_{30}$

[a] Frequencies from MP2(full)/6-31G(d) calculation. [b] Scaling factors of 0.88 for CH stretches, 1.0 for heavy atom bends, and 0.90 for all other modes. [c] Calculated infrared intensities in km/mol. [d] Calculated Raman activities in $Å^4$/u. [e] Values less than 10% are omitted. [f] * indicates carbon atom in the CH_2F group.

TABLE 4: Calculated Electronic Energies[a] (Hartree) and Energy Difference (cm^{-1}) for the Five Conformers of 4-Fluoro-1-butene

method/basis set	energy,[a] E *skew−gauche II*	energy difference,[b] ΔE *skew−trans*	*skew−gauche I*	*cis−trans*	*cis−gauche*
MP2/6-31G(d)	0.656956	194	278	541	316
MP2/6-31+G(d)	0.680724	102	209	593	505
MP2/6-311G(d,p)	0.901460	97	237	469	354
MP2/6-311+G(d,p)	0.912531	57	167	488	453
MP2/6-311G(2d,2p)	0.975433	98	228	342	202
MP2/6-311+G(2d,2p)	0.984337	33	143	315	298
MP2/6-311G(2df,2pd)	1.062752	82	203	306	189
MP2/6-311+G(2df,2pd)	1.070983	23	127	284	273
B3LYP/6-31G(d)	1.447345	104	279	421	298
B3LYP/6-31+G(d)	1.467302	−9	179	386	473
B3LYP/6-311G(d,p)	1.527590	78	237	401	319
B3LYP/6-311+G(d,p)	1.535475	2	144	362	422
B3LYP/6-311G(2d,2p)	1.537708	88	235	405	324
B3LYP/6-311+G(2d,2p)	1.544722	8	135	354	408
B3LYP/6-311G(2df,2pd)	1.543950	74	213	391	321
B3LYP/6-311+G(2df,2pd)	1.550946	1	123	344	401

[a] Energy of *skew−gauche II* conformer is given as −(*E*+255) H. [b] Difference is relative to *skew−gauche II* form.

of this study is that the conformer bands are better resolved in comparison with those in the infrared spectrum of the gas. From microwave studies[7,8] and *ab initio* calculations, the dipole moments of the five conformers are predicted to have similar values and the molecular sizes of the five rotamers are nearly the same, so the ΔH values obtained from the temperature-dependent FT-IR study are expected to be comparable to those for the gas.[16−20]

The intensities of several well-isolated and well-shaped conformational bands confidently assigned in the previous section were measured as a function of temperature (at 5.0 °C intervals between −115 and −155 °C), and their ratios were determined. By application of the van't Hoff equation $-\ln K = \Delta H/(RT) - \Delta S/R$, ΔH values were determined from plots of $-\ln K$ versus $1/T$, where $\Delta H/R$ are the slopes of the least-squares fitted lines and K values are substituted with the appropriate intensity ratios of pure conformer bands. It was assumed that the conformational enthalpy differences are not a function of temperature in the range studied.

Combining the two *skew−gauche II* bands at 850 and 965 cm^{-1} with the two *skew−trans* bands at 794 and 1061 cm^{-1}, the two *skew−gauche I* bands at 866 and 1027 cm^{-1}, the *cis−trans* band at 551 cm^{-1}, and the *cis−gauche* band at 529 cm^{-1} gave four pairs of bands that were utilized for the determination of the enthalpy differences among the three *skew* forms, and two pairs of bands were utilized to obtain the enthalpy differences between the *skew* and the *cis* forms. If one takes each conformer pair individually, there is a rather large variation in values, but taking the four band pairs as a single set gives a very small statistical uncertainty. From these data as a single set, an enthalpy difference of 72 ± 5 cm^{-1} (0.86 ± 0.06 $kJ\cdot mol^{-1}$) has been determined between the most stable *skew−gauche II* conformer and the second most stable *skew−trans* form. The third most stable conformer is the *skew−gauche I* with an enthalpy difference of 100 ± 7 cm^{-1} (1.20 ± 0.08 $kJ\cdot mol^{-1}$) compared with the most stable form. Larger enthalpy values of 251 ± 12 cm^{-1} (3.00 ± 0.14 $kJ\cdot mol^{-1}$) and 268 ± 17 cm^{-1} (3.21 ± 0.20 $kJ\cdot mol^{-1}$) were obtained for the *cis−trans* and *cis−gauche* conformers, respectively (Table 6). Although the statistical uncertainties are relatively small, they do not take into account possible contribution from combination or overtone bands from other conformers contributing to the measured fundamental band intensities. Thus, the realistic errors must be larger and probably as much 10% or possibly higher, but it is not possible to provide a confident estimate, so we are leaving the statistical values as the uncertainties. From these data and the relative statistical weights of one for the *cis−trans* conformer and two for all other forms, it is estimated that there are 36.4 ± 0.9% *skew−gauche II*, 25.7 ± 0.1% *skew−trans*, 22.5 ± 0.2% *skew−gauche I*, 10.0 ± 0.6% *cis−gauche*, and 5.4 ± 0.2% *cis−trans* forms (statistical uncertainties) present at ambient temperature (298 K). The statistical uncertainties are obviously too small and should be at least 2% for the conformers in greater abundance and 1% for those in smaller abundance.

Structural Parameters

In the initial microwave spectroscopic study[7] of 4-fluoro-1-butene in the frequency region 26.5−40.0 GHz, only the *skew−trans* rotamer was identified. Four years later, a second microwave investigation[8] in the frequency region 10.0−26.5 GHz identified three rotamers, *i.e.*, the *skew−gauche II*, *skew−trans*, and *skew−gauche I* forms. However, because only three rotational constants were available for the most abundant isotopic species of each conformer, only the two skeletal dihedral angles, CCC=C and FCCC, were fitted, with the rest of the structural parameters fixed at assumed values for all three forms. With eight assumed bond distances, nine assumed bond angles and an assumed strictly planar vinyl group, the resulting fit of the skeletal dihedral angles involve relatively large uncertainties and the tentatively proposed structures were less than satisfactory. Thus, we initiated a process to obtain more reliable structural parameters of the three *skew* conformers of 4-fluoro-1-butene.

First, we[21] have shown for more than fifty carbon−hydrogen distances that the r_e distances predicted from MP2(full)/6-311+G(d,p) calculations match the r_0 distances determined from the "isolated" CH stretching frequencies[22] to within ±0.002 Å. Considering this level of accuracy for the CH predicted distances as well as the small mass of the hydrogen atom, the effect on the rotational constants from the errors of the MP2(full)/6-311+G(d,p) predicted CH parameters are orders of magnitude smaller than those from the skeletal structure. It has also been shown[23] that similar calculations predict the CF distances very well for a large number of fluorocarbons. Finally, we have found[21] that we can obtain good structural parameters by adjusting the structural parameters obtained from the *ab initio* calculations to fit the rotational constants (computer program A&M, *Ab Initio* and Microwave, developed in our laboratory[24]) obtained from the microwave experimental data. To reduce the

TABLE 5: Structural Parameters (Å and Degree), Rotational Constants (MHz), and Dipole Moments (Debye) for the Three Skew Conformers of 4-Fluoro-1-butene

		skew−gauche II			*skew−trans*			*skew−gauche I*		
parameter	int coord	MP2/6-311+G(d,p)	microwave[a,b]	adjusted r_0	MP2/6-311+G(d,p)	microwave[a,b]	adjusted r_0	MP2/6-311+G(d,p)	microwave[a,b]	adjusted r_0
$r(C_1{=}C_2)$	R_1	1.340	1.331	1.343	1.340	1.331	1.341	1.339	1.331	1.338
$r(C_2{-}C_3)$	R_2	1.500	1.496	1.503	1.501	1.496	1.502	1.500	1.496	1.497
$r(C_3{-}C_4)$	R_3	1.517	1.530	1.516	1.518	1.530	1.519	1.517	1.530	1.517
$r(C_4{-}F_5)$	R_4	1.397	1.393	1.396	1.395	1.393	1.394	1.393	1.393	1.391
$r(C_1{-}H_6)$	r_1	1.087	1.090	1.087	1.087	1.090	1.087	1.086	1.090	1.086
$r(C_1{-}H_7)$	r_2	1.085	1.090	1.085	1.085	1.090	1.085	1.085	1.090	1.085
$r(C_2{-}H_8)$	r_3	1.088	1.090	1.088	1.090	1.090	1.090	1.090	1.090	1.090
$r(C_3{-}H_9)$	r_4	1.096	1.093	1.096	1.094	1.093	1.094	1.095	1.093	1.095
$r(C_3{-}H_{10})$	r_5	1.096	1.093	1.096	1.096	1.093	1.096	1.098	1.093	1.098
$r(C_4{-}H_{11})$	r_6	1.093	1.093	1.093	1.094	1.093	1.094	1.093	1.093	1.093
$r(C_4{-}H_{12})$	r_7	1.093	1.093	1.093	1.093	1.093	1.093	1.094	1.093	1.094
$\angle C_1{=}C_2C_3$	ψ_1	123.9	127.8	123.8	124.0	127.8	124.1	124.1	127.8	124.7
$\angle C_2C_3C_4$	ψ_2	112.3	111.6	113.0	110.6	111.6	110.8	112.6	111.6	113.5
$\angle C_3C_4F_5$	ψ_3	109.4	111.0	109.3	109.9	111.0	109.6	109.9	111.0	109.9
$\angle C_2{=}C_1H_6$	α_1	121.3	121.5	121.3	121.1	121.5	121.1	121.1	121.5	121.1
$\angle C_2{=}C_1H_7$	α_2	121.3	121.5	121.3	121.4	121.5	121.4	121.4	121.5	121.4
$\angle H_6C_1H_7$	α_3	117.4	117.0	117.4	117.5	117.0	117.5	117.5	117.0	117.5
$\angle C_1{=}C_2H_8$	β_1	119.6	121.5	119.6	119.1	121.5	119.1	119.3	121.5	119.3
$\angle C_3C_2H_8$	β_2	116.5		116.5	116.9		116.9	116.6		116.6
$\angle C_2C_3H_9$	ω_1	110.0		110.0	110.3		110.3	110.3		110.3
$\angle C_2C_3H_{10}$	ω_2	110.4		110.4	110.4		110.4	110.0		110.0
$\angle C_4C_3H_9$	θ_1	108.2	109.47	108.2	109.2	109.47	109.2	109.0	109.47	109.0
$\angle C_4C_3H_{10}$	θ_2	108.1	109.47	108.1	108.3	109.47	108.3	107.2	109.47	107.2
$\angle H_9C_3H_{10}$	δ_1	107.7	109.47	107.7	107.9	109.47	107.9	107.6	109.47	107.6
$\angle C_3C_4H_{11}$	ϵ_1	111.2	109.47	111.2	111.3	109.47	111.3	111.2	109.47	111.2
$\angle C_3C_4H_{12}$	ϵ_2	111.4	109.47	111.4	111.0	109.47	111.0	111.3	109.47	111.3
$\angle F_5C_4H_{11}$	π_1	107.4		107.4	107.5		107.5	107.4		107.4
$\angle F_5C_4H_{12}$	π_2	107.4		107.4	107.7		107.7	107.5		107.5
$\angle H_{11}C_4H_{12}$	δ_2	109.8	109.47	109.8	109.4	109.47	109.4	109.4	109.47	109.4
$\tau C_4C_3C_2{=}C_1$	τ_2	−119.3	−125(3)	−121.1	−113.1	−114(3)	−114.2	−117.9	−125(3)	−120.6
$\tau F_5C_4C_3C_2$	τ_1	−63.3	−63(3)	−63.3	−176.4	179(3)	−175.1	64.3	57(3)	63.7
$\tau H_9C_3C_2{=}C_1$	τ_2	1.2		1.2	7.9		7.9	4.1		4.1
$\tau H_{10}C_3C_2{=}C_1$	τ_2	120.0		120.0	127.1		127.1	122.6		122.6
$\tau H_{11}C_4C_3F_5$	τ_1	118.5		118.5	119.0		119.0	118.8		118.8
$\tau H_{12}C_4C_3F_5$	τ_1	−118.7		−118.7	−119.0		−119.0	−118.9		−118.9
$\tau H_6C_1{=}C_2C_3$	γ, η	−0.9	0	−0.9	−1.2	0	−1.2	−0.1	0	−0.1
$\tau H_7C_1{=}C_2C_3$	γ, η	179.3	180	179.3	179.2	180	179.2	179.4	180	179.4
$\tau H_8C_2{=}C_1C_3$	ξ	−179.2	180	−179.2	−179.0	180	−179.0	−179.3	180	−179.3
A		12865.9	13048.2161(61)	13047.4	19820.3	20089.510 (16)	20088.2	9809.2	10026.3189 (69)	10024.7
B		2660.1	2636.4673 (12)	2636.1	2137.9	2132.4569 (15)	2131.9	3086.9	3027.0373(19)	3026.1
C		2428.9	2406.3153 (11)	2406.5	2122.5	2112.5589 (15)	2112.6	2633.1	2601.3400(24)	2602.2
$\lvert\mu_a\rvert$		0.928	0.841(16)		1.985	1.62(1)[c]		0.298	0.332(6)	
$\lvert\mu_b\rvert$		1.842	1.458(22)		0.799	0.68(5)[c]		2.200	1.873(12)	
$\lvert\mu_c\rvert$		0.471	0.728(39)		0.041	0.39(14)[c]		0.191	0.090(30)	
$\lvert\mu_t\rvert$		2.115	1.835(33)		2.141	1.80(5)[c]		2.229	1.904(13)	

[a] Reference 8. All structural parameters reported were assumed except for $\tau C_4C_3C_2{=}C_1$ and $\tau F_5C_4C_3C_2$. [b] Differences in the *A*, *B*, and *C* of the experimental rotational constants and those obtained from the adjust r_0 parameters are: $\Delta A = 0.8$, $\Delta B = 0.4$, $\Delta C = 0.2$ for *skew−gauche II*; $\Delta A = 1.3$, $\Delta B = 0.6$, $\Delta C = 0.04$ for *skew−trans*; and $\Delta A = 1.6$, $\Delta B = 0.9$, $\Delta C = 0.9$ MHz for the *skew−gauche I* conformers. [c] Reference 7.

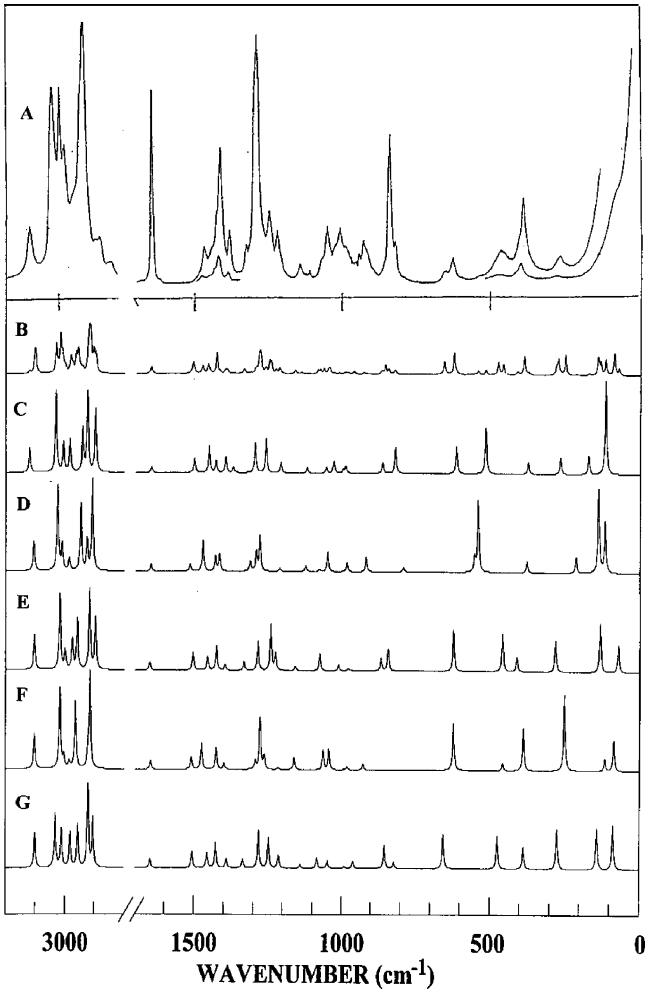

Figure 6. Raman spectra of 4-fluoro-1-butene: (A) liquid at room temperature; (B) simulated spectrum of a mixture of the five conformers at 25 °C with experimentally determined Δ*H* values listed in Table 6; (C) simulated spectrum for pure *cis*−*gauche* form; (D) simulated spectrum for pure *cis*−*trans* form; (E) simulated spectrum for pure *skew*−*gauche I* form; (F) simulated spectrum for pure *skew*−*trans* form; (G) simulated spectrum for pure *skew*−*gauche II* form.

number of independent variables, the structural parameters are separated into sets according to their types. Bond lengths in the same set keep their relative ratio, and bond angles and torsional angles in the same set keep their differences in degrees. This assumption is based on the fact that the errors from *ab initio* calculations are systematic. Additionally, we have also shown that the differences in predicted distances and angles from the *ab initio* calculations for different conformers of the same molecule can usually be used as one parameter with the *ab initio* predicted differences except for some dihedral angles. Therefore, it should be possible to obtain "adjusted r_0" structural parameters for 4-fluoro-1-butene from the nine determined rotational constants from the three skewed conformers. Thus, it is possible to reduce the number of independent structural parameters to nine (one CC bond length, one C=C distance, one CF distance, three skeletal angles, and three independent dihedral angles) by fixing the CH parameters at the MP2(full)/6-311+G(d,p) optimized values. These parameters are expected to be more accurate than those that could be obtained from an electron diffraction or microwave study alone.

These determined r_0 parameters are listed in Table 5 and the final fitting of the rotational constants is excellent with differences of 1.6 MHz for the A rotational constant for the *skew*−*gauche I* conformer and 1.3 MHz for this constant for

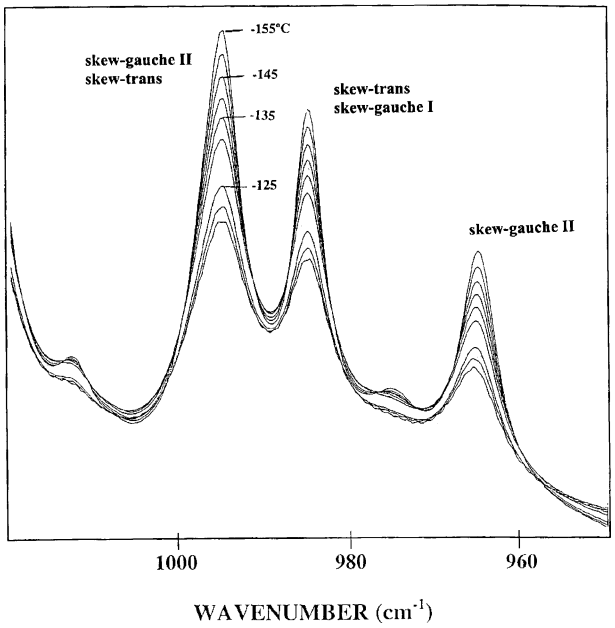

Figure 7. Temperature (−115 to −155 °C) dependence mid-infrared spectra in the 950−1200 cm^{-1} region of 4-fluoro-1-butene dissolved in liquid krypton.

the *skew*−*trans* conformer with the seven other rotational constants fit to better than 1 MHz (Table 5). The largest adjustments are associated with the three skeletal dihedral angles, the $C_4-C_3-C_2=C_1$ dihedral angle was adjusted from −119.3° to −121.1° for the *skew*−*gauche II* form, from −113.1° to −114.2° for the *skew*−*trans* form, and from −117.9° to −120.6° for the *skew*−*gauche I* form. Two of the $F_5-C_4-C_3-C_2$ dihedral angles had relatively small changes, from −176.4° to −175.1° for the *skew*−*trans* form and from 64.3° to 63.7° for the *skew*−*gauche I* form. It is somewhat difficult to estimate the uncertainties in these structural parameters, but it is believed those for CH distances should be no more than ±0.002 Å, the heavy atoms distances ±0.003 Å, and the angles ±0.5° except for the dihedral angles, which probably should be ±1.0°. Thus the adjusted r_0 parameters should be much more accurate than the estimated ones given in the previous microwave structural investigation[8] except for the values of the two heavy atom dihedral angles, which were obtained from the rotational data (Table 5). Even these two determined parameter values are very dependent on the values assumed for the other parameters.

To determine some structural parameters for comparison, we selected the 1-pentene molecule where the microwave spectra had been reported[5] for the normal molecule along with those for five isotopomers where each of the carbon atoms were substituted with ^{13}C. Therefore, eighteen rotational constants were reported[5] for the *skew*−*gauche I* with all having very small uncertainties. However for the *skew*−*gauche II* form five of the six A constants had significant uncertainties. For the *skew*−*trans* conformer all of the A constants have large uncertainties (Table 5S). Nevertheless, determined r_0 parameters could be obtained for each *skew* conformer individually by using the *ab initio* MP2(Full)/6-311+G(d,p) predicted parameters for the CH distances and angles and then obtaining the adjusted r_0 values for the remaining parameters. The fit of the constants that were well determined was excellent with most of them within 0.2 MHz (Table 5S).

The determined structural parameters for 1-pentene are listed in Table 7 along with the estimated uncertainties. These parameters clearly show the small changes in the heavy atom

TABLE 6: Temperature Dependent Intensity Ratios for the Five Conformers of 4-Fluoro-1-butene Dissolved in Liquid Krypton

T (°C)	$1000/T$ (K^{-1})	$I_{850sgII}/I_{794st}$	$I_{850sgII}/I_{1061st}$	$I_{965sgII}/I_{794st}$	$I_{965sgII}/I_{1061st}$	$I_{850sgII}/I_{866sgI}$	$I_{850sgII}/I_{1027sgI}$	$I_{965sgII}/I_{866sgI}$	$I_{965sgII}/I_{1027sgI}$	$I_{830sgII}/I_{551ct}$	$I_{474sgII}/I_{551ct}$	$I_{830sgII}/I_{529cg}$	$I_{474sgII}/I_{529cg}$
−115.0	6.3231	3.7946	0.12336	15.924	0.51767	0.42563	0.030268	1.7861	0.12702				
−120.0	6.5295	3.8765	0.12616	16.454	0.53550	0.43103	0.030459	1.8296	0.12929	1.1382	2.5349	1.9231	4.1803
−125.0	6.7499	3.9313	0.13309	16.571	0.56099	0.44099	0.032596	1.8589	0.13740	1.2701	2.7447	2.2150	4.5141
−130.0	6.9857	3.8226	0.13713	16.269	0.58359	0.45476	0.034231	1.9354	0.14569	1.4603	3.1656	2.4569	4.9667
−135.0	7.2385	4.1537	0.13983	17.900	0.60262	0.46472	0.036017	2.0027	0.15522	1.4679	3.4166	2.5883	5.0684
−140.0	7.5103	4.1331	0.14640	17.728	0.62796	0.47634	0.037264	2.0431	0.15983	1.6908	3.6418	3.0648	6.1569
−145.0	7.8034	4.2459	0.15401	17.842	0.64721	0.49605	0.041583	2.0845	0.17474	1.8150	3.9603	3.1882	7.1293
−150.0	8.1202	4.1640	0.15635	17.998	0.67580	0.49053	0.041497	2.1203	0.17937	1.9701	4.3636	3.2689	7.3255
−155.0	8.4638	4.4986	0.16004	19.369	0.68905	0.50636	0.044917	2.1801	0.19339				
ΔH (cm^{-1})		49 ± 8	88 ± 5	56 ± 8	95 ± 5	58 ± 4	114 ± 7	66 ± 4	140 ± 5	251 ± 19	251 ± 16	253 ± 29	282 ± 17
overall ΔH (cm^{-1})[a]			72 ± 5[a]			100 ± 7[b]				251 ± 12[c]		268 ± 17[d]	

[a] Value obtained by utilizing ΔH data of columns 3-6. [b] Value obtained by utilizing ΔH data of columns 7-10. [c] Value obtained by utilizing ΔH data of columns 11 and 12. [d] Value obtained by utilizing ΔH data of columns 13 and 14.

distances and angles that are needed to fit the large number of rotational constants, which gives confidence to the small uncertainties estimated for the determined parameters for the 4-fluorobutene molecule.

Discussion

Two scaling factors of 0.88 and 0.90 have been used with the MP2(full)/6-31G(d) calculations to obtain the predicted vibrational frequencies, which are in good agreement with the observed values. The average error in the frequency predictions for the normal modes of the most stable *skew−gauche II* conformer is 12 cm^{-1}, which represents a relative error of only 0.8%. For the *skew−trans* conformer, the average error in the frequency predictions for the normal modes is 14 cm^{-1}, which represents a relative error of less than 1.0%. For the *skew−gauche I* conformer, the average error in the frequency predictions for the normal modes is 13 cm^{-1}, which represents a relative error of 0.9%. Thus, multiple scaling factors are not necessary for predicting the frequencies of normal modes, particularly, for distinguishing those for the different conformers.

Because most of the structural parameters for the five conformers differ very little, most of the corresponding force constants are nearly the same from scaled MP2(full)/6-31G(d) results (Table 3S). The largest force constant differences among the five forms are associated with the heavy atom bending and torsional modes. The $C_1{=}C_2C_3$ bending force constants are nearly the same for all three *skew* forms; however, those of the *cis−trans* and *cis−gauche* forms are 14% and 28% larger, respectively. Similarly, the $C_2C_3C_4$ bending force constants are significantly larger for the two *cis* forms compared with the three *skew* forms, in particular, the one of the *cis−gauche* form (1.013 mdyn·Å·rad^{-2}) is 55% larger than the one of the *skew−trans* form (0.655 mdyn·Å·rad^{-2}). In addition, the $C_1{=}C_2H_8$ and the $C_3C_2H_8$ bending force constants are also noticeably larger for the two *cis* forms.

A comparison of the experimentally determined conformational enthalpy differences with the theoretical predictions shows that second-order Møller−Plesset perturbation theory[12] calculation with the largest diffuse-function-inclusive basis set utilized (MP2(full)/6-311+G(2df,2pd) provides the closest predictions. The inclusion of diffuse functions significantly lowers the predicted energies of the FCCC *trans* orientation and raises the energies of the FCCC *gauche* orientation. According to the previous microwave investigation,[8] the *skew−trans* and the *skew−gauche I* forms were determined to be less stable than the *skew−gauche II* form by 1.9 ± 0.2 kJ·mol^{-1} (159 ± 17 cm^{-1}) and 2.1 ± 0.2 kJ·mol^{-1} (176 ± 17 cm^{-1}), respectively. Although this determined conformational stability order of the three *skew* forms agrees with the present study, the enthalpy differences are almost twice the values we obtained from the present study, *i.e.*, 72 ± 7 cm^{-1} (0.86 ± 0.08 kJ·mol^{-1}) and 100 ± 10 cm^{-1} (1.20 ± 0.12 kJ·mol^{-1}), respectively. Support for the significantly small values is obtained from the *ab initio* calculations with the three largest basis sets utilized where the average value of 68 cm^{-1} without diffuse functions (37 cm^{-1} with diffuse functions) for the energy difference between the *skew−trans* and *skew−gauche II* forms. The largest basis set with diffuse function utilized in the calculations also supports the smaller enthalpy value between the *skew−gauche I* and *skew−gauche II* conformers with the predicted value of 127 cm^{-1} for the energy difference. Additional support for the smaller values is also found by using the predicted intensity values for several bands of the different conformers and their relative intensities.

TABLE 7: Structural Parameters (Å and Degree) for the Three Skew Conformers of 1-Pentene

	skew−gauche II		*skew−trans*		*skew−gauche I*	
parameters	MP2/6-311+G(d,p)	adjusted r_0	MP2/6-311+G(d,p)	adjusted r_0	MP2/6-311+G(d,p)	adjusted r_0
$r(C_1{=}C_2)$	1.341	1.344(3)	1.341	1.342(3)	1.341	1.340(3)
$r(C_2{-}C_3)$	1.501	1.503(3)	1.499	1.500(3)	1.500	1.497(3)
$r(C_3{-}C_4)$	1.536	1.534(3)	1.533	1.534(3)	1.535	1.536(3)
$r(C_4{-}C_5)$	1.527	1.525(3)	1.527	1.528(3)	1.526	1.526(3)
$r(C_1{-}H_6)$	1.087	1.087(2)	1.087	1.087(2)	1.087	1.087(2)
$r(C_1{-}H_7)$	1.085	1.085(2)	1.085	1.085(2)	1.085	1.085(2)
$r(C_2{-}H_8)$	1.089	1.089(2)	1.091	1.091(2)	1.091	1.091(2)
$r(C_3{-}H_9)$	1.096	1.096(2)	1.097	1.097(2)	1.097	1.097(2)
$r(C_3{-}H_{10})$	1.098	1.098(2)	1.098	1.098(2)	1.097	1.097(2)
$r(C_4{-}H_{11})$	1.096	1.096(2)	1.097	1.097(2)	1.096	1.096(2)
$r(C_4{-}H_{12})$	1.096	1.096(2)	1.096	1.096(2)	1.097	1.097(2)
$r(C_5{-}H_{13})$	1.093	1.093(2)	1.093	1.093(2)	1.094	1.094(2)
$r(C_5{-}H_{14})$	1.095	1.095(2)	1.094	1.094(2)	1.093	1.093(2)
$r(C_5{-}H_{15})$	1.093	1.093(2)	1.094	1.094(2)	1.095	1.095(2)
$\angle C_1{=}C_2C_3$	123.9	123.8(5)	124.4	124.6(5)	124.8	125.3(5)
$\angle C_2C_3C_4$	113.1	113.7(5)	112.3	112.5(5)	112.4	113.4(5)
$\angle C_3C_4C_5$	113.3	114.0(5)	112.4	112.5(5)	112.7	113.2(5)
$\angle C_2{=}C_1H_6$	121.1	121.1(5)	121.1	121.1(5)	121.0	121.0(5)
$\angle C_2{=}C_1H_7$	121.5	121.5(5)	121.5	121.5(5)	121.5	121.5(5)
$\angle H_6C_1H_7$	117.4	117.4(5)	117.5	117.5(5)	117.5	117.5(5)
$\angle C_1{=}C_2H_8$	118.7	118.7(5)	119.0	119.0(5)	118.9	118.9(5)
$\angle C_3C_2H_8$	117.3	117.3(5)	116.5	116.5(5)	116.3	116.3(5)
$\angle C_2C_3H_9$	109.0	109.0(5)	109.5	109.5(5)	109.5	109.5(5)
$\angle C_2C_3H_{10}$	109.5	109.5(5)	109.6	109.6(5)	109.1	109.1(5)
$\angle C_4C_3H_9$	109.4	109.4(5)	109.5	109.5(5)	109.5	109.5(5)
$\angle C_4C_3H_{10}$	108.6	108.6(5)	108.7	108.7(5)	109.0	109.0(5)
$\angle H_9C_3H_{10}$	107.1	107.1(5)	107.1	107.1(5)	107.2	107.2(5)
$\angle C_3C_4H_{11}$	108.7	108.7(5)	109.1	109.1(5)	108.8	108.8(5)
$\angle C_3C_4H_{12}$	108.6	108.6(5)	108.7	108.7(5)	109.1	109.1(5)
$\angle C_5C_4H_{11}$	109.8	109.8(5)	109.8	109.8(5)	109.6	109.6(5)
$\angle C_5C_4H_{12}$	109.3	109.3(5)	110.0	110.0(5)	109.8	109.8(5)
$\angle H_{11}C_4H_{12}$	106.9	106.9(5)	106.7	106.7(5)	106.7	106.7(5)
$\angle C_4C_5H_{13}$	111.0	111.0(5)	111.4	111.4(5)	111.2	111.2(5)
$\angle C_4C_5H_{14}$	110.7	110.7(5)	110.7	110.7(5)	111.1	111.1(5)
$\angle C_4C_5H_{15}$	111.5	111.5(5)	110.8	110.8(5)	110.5	110.5(5)
$\angle H_{13}C_5H_{14}$	107.9	107.9(5)	108.0	108.0(5)	108.2	108.2(5)
$\angle H_{13}C_5H_{15}$	107.6	107.6(5)	108.0	108.0(5)	108.0	108.0(5)
$\angle H_{14}C_5H_{15}$	108.0	108.0(5)	107.8	107.8(5)	107.7	107.7(5)
$\tau C_4C_3C_2{=}C_1$	−111.6	−115.4	−116.2	−118.6	−118.3	−119.2
$\tau C_5C_4C_3C_2$	−62.7	−63.7	−178.3	−178.1	64.2	64.5
$\tau H_9C_3C_2{=}C_1$	10.2	10.2	5.7	5.7	3.7	3.7
$\tau H_{10}C_3C_2{=}C_1$	127.1	127.1	122.9	122.9	120.7	120.7
$\tau H_{11}C_4C_3C_5$	122.4	122.4	122.0	122.0	121.8	121.8
$\tau H_{12}C_4C_3C_5$	−121.7	−121.7	−122.1	−122.1	−122.2	−122.2
$\tau H_6C_1{=}C_2C_3$	−1.1	−1.1	−1.4	−1.4	−0.5	−0.5
$\tau H_7C_1{=}C_2C_3$	179.0	179.0	178.7	178.7	179.6	179.6
$\tau H_8C_2{=}C_1C_3$	−179.4	−179.4	−178.5	−178.5	−179.3	−179.3
$\tau H_{13}C_5C_4C_3$	−175.5	−175.5	−179.6	−179.6	178.8	178.8
$\tau H_{14}C_5C_4C_3$	−55.7	−55.7	−59.4	−59.4	−60.6	−60.6
$\tau H_{15}C_5C_4C_3$	65.5	65.5	60.1	60.1	58.8	58.8

TABLE 8: Calculated and Experimental Centrifugal Distortion Constants (in kHz) of the *Skew−Gauche II*, *Skew−Trans*, and *Skew−Gauche I* Conformers of 4-Fluoro-1-butene in the Ground Vibrational State

	skew−gauche II		*skew−trans*		*skew−gauche I*	
	MP2(full)/6-311+G(d,p)	exptl[a]	MP2(full)/6-311+G(d,p)	exptl[a]	MP2(full)/6-311+G(d,p)	exptl[a]
Δ_J	1.906	1.9979(23)	0.6598	0.755(12)	4.859	5.025(14)
Δ_K	176.594	206.370(45)	471.222		94.671	130.727(37)
Δ_{JK}	−27.455	−31.813(30)	−23.330	−26.165(29)	−30.345	−41.44(12)
δ_J	0.187	0.21429(33)	−0.1077	−0.128432(40)	1.424	1.5184(44)
δ_K	4.781	5.158(98)	81.246		8.452	7.84(22)

[a] Reference 8.

Five centrifugal distortion constants, Δ_J, Δ_K, Δ_{JK}, δ_J, and δ_K, were calculated with the Gaussian 03 software package[10] for all three *skew* conformers, and they are listed in Table 8. However, only the Δ_J, Δ_{JK}, and δ_J values were experimentally determined[8] for the *skew−trans* form because this rotamer is nearly a prolate rotor ($\kappa = -0.998$) and they agree favorably with the predicted values. For the *skew−gauche II* and *skew−gauche I* rotamers, all five of the centrifugal distortion constants were experimentally determined and the agreement between the predicted and experimental values is quite good. The poorest agreement seems to be with the relatively large Δ_K constant. Nevertheless, these limited results suggest that *ab initio* calculations at the MP2(full)/6-311+G(d,p) level provide satisfactory predictions of the centrifugal distortion constants of 4-mono-

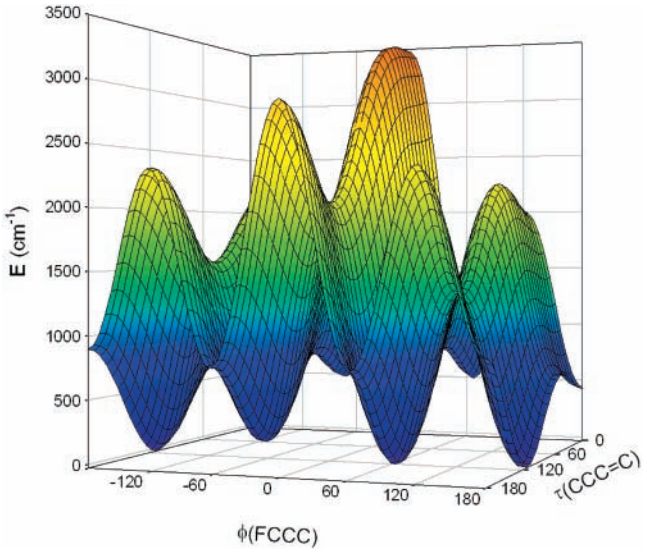

Figure 8. Theoretical potential surface governing τ(CCC═C) and ϕ-(FCCC) torsions in 4-fluoro-1-butene, calculated at MP2(full)/6-311+G-(d,p) level.

substituted-1-butene molecules and it is probable that even the smaller basis set of 6-31G(d) would give very reasonable values.

The conformational interchange of 4-fluoro-1-butene involves the τ(CCC═C) and the ϕ(FCCC) dihedral angles. In the context of our conformational energetics study, the potential energy of the molecule is a function of these two dihedral angles, τ and ϕ. The resulting three-dimensional potential surface is shown in Figure 8. The most stable *skew−gauche II* conformer ($\tau \approx 120°$, $\phi \approx 60°$) corresponds to the global minimum whereas the less stable *skew−trans* ($\tau \approx 120°$, $\phi \approx 180°$), *skew−gauche I* ($\tau \approx 120°$, $\phi \approx -60°$), *cis−trans* ($\tau = 0°$, $\phi = 180°$) and *skew−gauche* ($\tau \approx 0°$, $\phi \approx \pm 60°$) conformers corresponds to local minima. The *cis−skew*, *trans−trans*, *trans−gauche*, *skew−cis*, *skew−skew I* and *II*, *gauche−cis*, and *gauche−gauche I* and *II* forms correspond to first-order saddle points. The global maximum corresponds to the *cis−cis* form and *trans−cis*, *trans−skew*, *gauche−trans*, and *gauche−skew I* and *II* forms are local maxima. Both cross-sections of the potential surfaces along the τ(CCC═C) and the ϕ(FCCC) dihedral angles are 3-fold. In addition, the function describing the potential energy surface, $E(\tau,\phi)$, must conform to the following symmetry restrictions $E(\tau,\phi) = E(-\tau,-\phi) \neq E(-\tau,\phi) = E(\tau,-\phi)$. Thus, by applying the common approach of fitting Fourier series to represent two-dimensional potential curves, the three-dimensional surface should take on the general form of

$$E(\tau,\phi) = {}^1/_2\sum_i [V_{i0} + {}^1/_2\sum_j V_{ij}(1 - \cos j\phi)](1 - \cos i\tau) + {}^1/_4\sum_i\sum_j V'_{ij} \sin j\phi \sin i\tau + {}^1/_2\sum_j V_{0j}(1 - \cos j\phi) + V_{00}$$

where the first term is the Fourier cosine series of τ, describing the potential curve along the τ(CCC═C) dihedral. The Fourier cosine coefficients are a function of the ϕ(FCCC) dihedral, and they are fitted by another Fourier cosine series of ϕ. Similarly, the second term is the Fourier sine series of the τ(CCC═C) dihedral where the sine coefficients are now fitted by another Fourier sine series of the ϕ(FCCC) dihedral. The third term describes the symmetric potential curve as a function of the ϕ(FCCC) dihedral, along the τ(CCC═C) = 0 (*cis*) cross-section. The last term, V_{00}, is a constant equal to the energy difference between the *cis−cis* ($\tau = f = 0$, global maximum) and the most stable *skew−gauche II* conformations.

TABLE 9: Calculated (MP2(full)/6-311+G(d,p)) Fourier Coefficients of the Potential Surface for the Two-Dimensional Conformational Interchange of 4-Fluoro-1-butene

Fourier Cosine Series Coefficients (cm^{-1})						
V_{10}	−1167	V_{11}	818	V_{21}	64	V_{31}	−6
V_{20}	−726	V_{12}	428	V_{22}	282	V_{32}	53
V_{30}	503	V_{13}	291	V_{23}	147	V_{33}	20
Fourier Sine Series Coefficients (cm^{-1})						
		V'_{11}	−251	V'_{21}	296	V'_{31}	−10
		V'_{12}	19	V'_{22}	−136	V'_{32}	−10
		V'_{13}	−338	V'_{23}	−153	V'_{33}	−190
Energy Correction Coefficients (cm^{-1})						
V_{00}	3469	V_{01}	−1084	V_{02}	−894	V_{03}	−1950

Our analysis shows that for the 3-fold potential along the τ(CCC═C) and ϕ(FCCC) dihedrals, only the first three Fourier cosine and sine terms are significant. Thus, the potential surface, $E(\tau,\phi)$, can be reduced to the following form:

$$E(\tau,\phi) = {}^1/_2\sum_{i=1}^{3} [V_{i0} + {}^1/_2\sum_{j=1}^{3} V_{ij}(1 - \cos j\phi)](1 - \cos i\tau) + {}^1/_4\sum_{i=1}^{3}\sum_{j=1}^{3} V'_{ij} \sin j\phi \sin i\tau + {}^1/_2\sum_{j=1}^{3} V_{0j}(1 - \cos j\phi) + V_{00}$$

The resulting least-squares-fitted potential coefficients, fitted from the calculated electronic energies at the MP2(full)/6-311+G(d,p) level, for the two-dimensional conformational interchange of 4-fluoro-1-butene are listed in Table 9.

For 4-fluoro-1-butene, the three *skew* conformers are determined to be more stable than the two *cis* forms, suggesting that the steric effect is the predominant factor in deciding the orientation along the (C═)C−C(−C) bond. The same order of stability is found in most monosubstituted allyl molecules, CH_2═$CHCH_2X$ where the *gauche* conformer is more stable than the *cis* form. For the prediction of the preferred orientation along the (C−)C−C(−F) bond, there should be a good correlation between the conformational stability of our target compound and that of 1-fluoropropane.[25−28] For this latter molecule the *gauche* conformer is more stable than the *trans* form by about 100 cm^{-1}; thus, one expects the *skew−gauche* conformers of 4-fluoro-1-butene to be more stable than the *skew−trans* form, which agrees with the experimental results. The *skew−*gauche I conformer could have some steric interaction to cause it to be less stable than the *skew−trans* form. With these arguments, it seems doubtful that the *cis−trans* conformer is the most stable form of 3-butenylsilane[6] (CH_2═$CHCHCHSiH_3$). It should be noted that the variable temperature Raman spectroscopic study was carried out with the sample in the liquid phase.[6] However, because the molecule is expected to have a relatively small permanent dipole, the relatively weak molecular association should not significantly affect the relative conformational stability. Thus, another conformational determination of 3-butenylsilane would be of interest.

Acknowledgment. J.R.D. acknowledges the University of Missouri−Kansas City for a Faculty Research Grant for partial financial support of this research.

Supporting Information Available: Table 1S, observed and calculated frequencies and potential energy distributions for the *cis−trans* conformer at MP2(full)/6-31G(d) *ab initio* calculation for 4-fluoro-1-butene and Table 2S similar information for the *cis−gauche*. Table 3S, scaled diagonal force constants from

MP2(full)/6-31G(d) *ab initio* calculations for 4-fluoro-1-butene; Table 4S, symmetry coordinates for 4-fluoro-1-butene; Table 5S, predicted (MP2(full)/6-311+G(d,p)) and experimental rotational constants (MHz) for the three skew conformers of six isotopomers of 1-pentene along with their values from the adjusted r_0 parameters; Figure 1S, far-infrared spectrum of gaseous 4-fluoro-1-butene; Figure 2S, infrared spectra of 4-fluoro-1-butene: (A) krypton solution at −130 °C (B) simulated spectra of a mixture of the five conformers; Figure 3S, atom numbering of the stable *skew−gauche II*, *skew−trans*, and *skew−gauche I* conformers of 1-pentene. This material is available free of charge *via* the Internet at http://pubs.acs.org.

References and Notes

(1) Kondo, S.; Hirota, E.; Morino, Y. *J. Mol. Spectrosc.* **1968**, *28*, 471.
(2) Van Hemelrijk, D.; Van den Enden, L.; Geise, H. J.; Sellers, H. L.; Schaefer, L. *J. Am. Chem. Soc.* **1980**, *102*, 2189.
(3) Bell, S.; Drew, B. R.; Guirgis, G. A.; Durig, J. R. *J. Mol. Struct.* **2000**, *553*, 199.
(4) Schei, S. H. *J. Mol. Struct.* **1985**, *128*, 151.
(5) Fraser, G. T.; Xu, L. -H.; Suenram, R. D.; Lugez, C. L. *J. Chem. Phys.* **2000**, *112*, 6209.
(6) Taga, K.; Ohno, K.; Murata, H. *Bull. Chem. Soc. Jpn.* **1979**, *52*, 1279.
(7) Li, Y. S.; Liu, B. Y.; Guirgis, G. A. *J. Mol. Struct.* **1987**, *162*, 305.
(8) Guirgis, G. A.; Marstokk, K. M.; Møllendal, H. *Acta Chem. Scand.* **1991**, *45*, 482.
(9) Furic, K.; Durig, J. R. *Appl. Spectrosc* **1988**, *42*, 175.
(10) Frisch, M. J.; Trucks, G. W.; Schlegel, H. B.; Scuseria, G. E.; Robb, M. A.; Cheeseman, J. R.; Montgomery, J. A., Jr; Vreven, T.; Kudin, K. N.; Burant, J. C.; Millam, J. M.; Iyengar, S. S.; Tomasi, J.; Barone, V.; Mennucci, B.; Cossi, M.; Scalmani, G.; Rega, N.; Petersson, G. A.; Nakatsuji, H.; Hada, M.; Ehara, M.; Toyota, K.; Fukuda, R.; Hasegawa, J.; Ishida, M.; Nakajima, T.; Honda, Y.; Kitao, O.; Nakai, H.; Klene, M.; Li, X.; Knox, J. E.; Hratchian, H. P.; Cross, J. B.; Adamo, C.; Jaramillo, J.; Gomperts, R.; Stratmann, R. E.; Yazyev, O.; Austin, A. J.; Cammi, R.; Pomelli, C.; Ochterski, J. W.; Ayala, P. Y.; Morokuma, K.; Voth, G. A.; Salvador, P.; Dannenberg, J. J.; Zakrzewski, V. G.; Dapprich, S.; Daniels, A. D.; Strain, M. C.; Farkas, O.; Malick, D. K.; Rabuck, A. D.; Raghavachari, K.; Foresman, J. B.; Ortiz, J. V.; Cui, Q.; Baboul, A. G.; Clifford, S.; Cioslowski, J.; Stefanov, B. B.; Liu, G.; Liashenko, A.; Piskorz, P.; Komaromi, I.; Martin, R. L.; Fox, D. J.; Keith, T.; Al-Laham, M. A.; Peng, C. Y.; Nanayakkara, A.; Challacombe, M.; Gill, P. M. W.; Johnson, B.; Chen, W.; Wong, M. W.; Gonzalez, C.; Pople, J. A. *Gaussian 03*, revision B.04; Gaussian, Inc.: Pittsburgh, PA, 2003.
(11) Pulay, P. *Mol. Phys.* **1969**, *179*, 197.
(12) Møller, C.; Plesset, M. S. *Phys. Rev.* **1934**, *46*, 618.
(13) Becke, A. D. *J. Chem. Phys.* **1993**, *98*, 5648.
(14) Lee, C.; Yang, W.; Parr, R. G. *Phys. Rev. B* **1988**, *37*, 785.
(15) Gurigis, G. A.; Zhu, X.; Yu, Z.; Durig, J. R. *J. Phys. Chem. A* **2000**, *104*, 4383.
(16) Herrebout, W. A.; van der Veken, B. J. *J. Phys. Chem.* **1996**, *100*, 9671.
(17) Herrebout, W. A.; van der Veken, B. J.; Wang, A.; Durig, J. R. *J. Phys. Chem.* **1995**, *99*, 578.
(18) Bulanin, M. O. *J. Mol. Struct.* **1995**, *347*, 73.
(19) van der Veken, B. J.; DeMunck, F. R. *J. Chem. Phys.* **1992**, *97*, 3060.
(20) Bulanin, M. O. *J. Mol. Struct.* **1973**, *19*, 59.
(21) Durig, J. R.; Ng, K. W.; Zheng, C.; Shen, S. *Struct. Chem.* **2004**, *5*, 149.
(22) McKean, D. C.; Torto, I. *J. Mol. Struct.* **1982**, *81*, 51.
(23) Villamanan, R. M.; Chen, W. D.; Wlodarczak, G.; Demaison, J.; Lesarri, A. G.; Lopez, J. C.; Alonso, J. L. *J. Mol. Spectrosc.* **1995**, *171*, 223.
(24) Van der Veken, B. J.; Herrebout, W. A.; Durig, D. T.; Zhao, W.; Durig, J. R. *J. Phys. Chem. A* **1999**, *103*, 1976.
(25) Guirgis, G. A.; Zhu, X.; Durig, J. R. *Struct. Chem.* **1999**, *10*, 445.
(26) Hirota, E. *J. Chem. Phys.* **1962**, *37*, 283.
(27) Durig, J. R.; Godbey, S. E.; Sullivan, J. F. *J. Chem. Phys.* **1984**, *80*, 5983.
(28) Goodman, L.; Sauers, R. R. *J. Chem. Theory Comput.* **2005**, *1*, 1185.